17th World Conference on Earthquake Engineering, 17WCEE
Sendai, Japan - September 13th to 18th 2020
Paper N° C000007
Registration Code: S-A00508

PHAETHON: SOFTWARE FOR ANALYSIS OF SHEAR-CRITICAL REINFORCED CONCRETE COLUMNS

K.G. Megalooikonomou [1]

[1] *Research Engineer, German Research Centre for Geosciences (GFZ), Helmholtz Centre Potsdam, kmegal@gfz-potsdam.de*

Abstract

Earthquake collapse of substandard reinforced concrete (RC) buildings, designed and constructed before the development of modern seismic design Codes, has triggered intense efforts by the scientific community for accurate assessment of this building stock. Most of the proposed procedures for the prediction of building strength and deformation indices were validated by assembling databases of RC column specimens tested under axial load and reversed cyclic lateral drift histories. Usually a column structural behavior is assessed by considering all involving mechanisms of behavior, namely flexure with or without the presence of axial load, shear and anchorage. In the present paper a force-based fiber beam/column element was developed accounting for shear and tension stiffening effects in order to provide an analytical test-bed for simulation of experimental cases such as the lightly reinforced columns forced to collapse. Their peculiar characteristics are the outcome of the shear – flexure interaction mechanism modeled here based on the Modified Compression Field Theory (MCFT) and the significant contribution of the tensile reinforcement pull-out from its anchorage to the total column's lateral drift. These features are embedded in this first-proposed stand-alone Windows program named "Phaethon" -with user's interface written in C++ programming language code- aiming to facilitate engineers in executing analyses both for rectangular and circular substandard RC columns.

Keywords: shear-critical columns; MCFT; anchorage pull-out; fiber beam/column element; capacity curve

1. Introduction

Even the most advanced stage of development on seismic design and assessment to date requires some kind of nonlinear analysis - either static or dynamic. Such investigations are mostly carried out using frame elements with different levels of approximation. Two main approaches are mostly used, classified as lumped-plasticity and distributed-inelasticity models. The limitation of lumped plasticity elements is that inelastic deformations take place at predetermined locations in the ends of the element. Another, in many respects more serious limitation, is the fact that lumped plasticity elements require calibration of their parameters against the response of an actual or ideal frame element under idealized loading conditions. This is necessary, because the response of concentrated plasticity elements derives from the moment–rotation relation of their components. In an actual frame element, the end moment–rotation relation results from the integration of the section response. This can be achieved directly with elements of distributed inelasticity ([1], [2]). For the latter approach, the so-called fiber beam elements (Fig. 1) provide results that seem to be particularly appropriate for studying the behavior of reinforced concrete (RC) structures under reversed cyclic loads: moment-axial force (M-N) coupling is readily taken into account, as well as the interaction between concrete and steel in the section. Whereas a few fiber beam-column elements have been developed with good capability of reproducing axial force and flexure effects, on the other hand, the coupling between the effects of normal and shear forces is not straightforward and hence only a few modelling strategies have accounted for, and were fully implemented up till now [3].

A common framework, appropriate for the analysis of beam-column elements, is the Euler-Bernoulli approach. The fundamental kinematic assumption is that cross-sections remain plain and normal to the deformed longitudinal axis. The engineering beam theory reproduces the response of a beam under combined axial force and bending moments, while shear forces are recovered from a static equilibrium; the effects of shear on beam's deformation are neglected. Where the effects of tangential stresses are important for the element deformation (i.e. in a beam-columns joint or in the column/wall plastic hinge length), more refined theories like the Timoshenko beam theory may be used for modeling the member deformation response.

In the development of a nonlinear frame element, two main approaches have been used, namely the displacement-based (stiffness) approach and the force-based (flexibility) approach. The flexibility-based frame element gives the exact solutions for non-linear analysis of frame structures using force interpolation functions that strictly satisfy element equilibrium, and impose the compatibility conditions. Accordingly, this approach allows the overcoming of some limitations of the stiffness approach. In particular, the nonlinear analysis becomes independent of the displacement approximation, it requires fewer elements for the representation of the non-linear behavior and, above all, in the case of a Timoshenko element or exact-beam theory-element, it avoids the well-known shear-locking problem (a sharp increase in the element stiffness which results in far fewer deformations for the element than expected) [4].

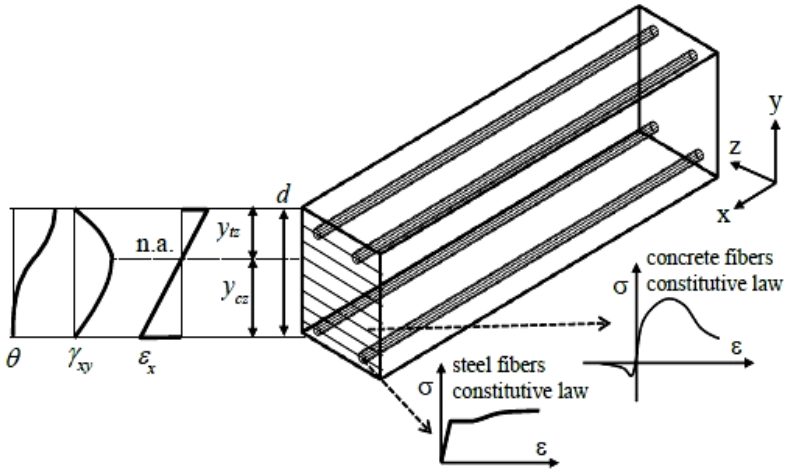

Fig. 1 – Fiber Element Scheme – definitions [5], [6].

A pre-requisite for incorporating the Timoshenko beam theory (i.e. accounting for shear) into the fiber approach, is the use of pertinent constitutive relationships. This includes fiber beam-column elements using smeared cracking models. According to this approach, cracked concrete is simulated as a continuous medium with anisotropic characteristics. In general, these models are referred to as "smeared cracking approaches" since cracking is modelled as a distributed effect with directionality. These approaches are particularly suitable for sectional analysis.

2. RC Sectional Model Based on Modified Compression Field Theory (MCFT)

Since the end of 1970s, a considerable amount of experimental and analytical research has been conducted with the aim of developing analytical procedures capable of estimating the load-deformation response of reinforced concrete elements loaded in shear [7]. At the University of Toronto, Collins developed a procedure called the compression field theory (CFT) in 1978 [8]. In 1981, a competition was held to predict the load-deformation response of four reinforced concrete panels tested at the University of Toronto [9], where leading researchers from around the world entered predictions based on various constitutive approaches. The results indicated that the most highly developed level in analytical modelling at the time was far from satisfactory. Generally, the models were not able to adequately estimate the ultimate strength, the failure mode or the load-deformation response of the panels. Most of the entrants used constitutive theories developed from tests conducted on plain concrete specimens; these do not account effectively for the modification of the properties of concrete after cracking, that is owing to the interaction between the concrete and steel that governs the response of reinforced concrete structures. In an effort to determine more realistic relationships for cracked reinforced concrete, Vecchio and Collins [10] tested a series of RC panels. From these tests, the modified compression field theory (MCFT) [11] was calibrated by including stress-strain relationships for cracked reinforced concrete under plane stress conditions.

An RC element is homogenized and is treated as anisotropic elastic material shown in Fig.2. Consider an elementary panel under constant plane stress, of uniform thickness, containing a rectangular grid of well distributed reinforcement. Loads acting on the element's edge planes are assumed to consist of uniform membrane stresses, i.e., axial stresses n_x, n_y and uniform shear stresses τ_{xy}. The deformed shape is defined by the strain tensor for plane stresses:

$$\begin{bmatrix} \varepsilon_x & \gamma_{xy}/2 & 0 \\ \gamma_{xy}/2 & \varepsilon_y & 0 \\ 0 & 0 & \varepsilon_z \end{bmatrix} \quad (1)$$

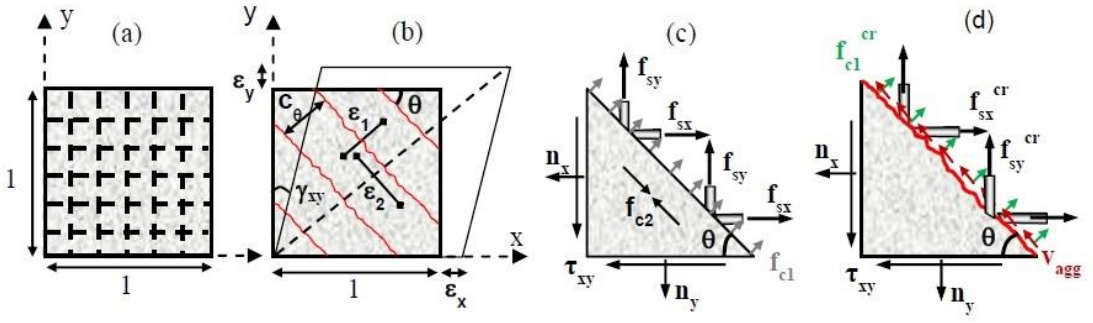

Fig. 2 – a) RC smeared-cracking membrane element, b) average strains (C_θ: spacing of cracks inclined at θ) c) average stresses and d) local stresses [5], [6].

The MCFT utilizes the following assumptions:

- The reinforcement is averaged or smeared throughout the element, i.e. the theory applies only to adequately-detailed members.
- The stresses applied to the element are uniform along edges.
- The total stress state is a function of the total strain state.
- The reinforcement is perfectly bonded to concrete, so that relative displacement due to bond slip between reinforcement and concrete is ignored.
- The shear stress in reinforcement is neglected.
- The principal stresses and principal strain axes are coincident; as a consequence, no deviation between the two is allowed.
- The constitutive relationships for concrete and reinforcement are independent.
- The cracks are smeared and allowed to rotate.

The theory comprises three sets of relationships: compatibility relationships between average strains of concrete and reinforcement, equilibrium relationships between externally applied loads and average stresses in the concrete and reinforcement; and uniaxial stress-strain relationships for cracked concrete along the principal directions and for reinforcement. The constitutive relationships for cracked concrete result from tests of reinforced concrete panels using a purpose-built Panel Element Tester at the University of Toronto. As such, the formulation of the MCFT calibrated with the specific tests conducted in the panel tester, incorporates realistic constitutive models for concrete based on experimentally observed phenomena. While cracks are smeared and the relationships are formulated in terms of average stresses and strains, a critical aspect of the MCFT is the consideration of the local strain and stress conditions at cracks (Fig.2d).

2.1 Constitutive Model based on MCFT for a Fiber RC Beam

In order to determine the normal and the shear stresses for the *i*-th fiber/layer (σ_x^i, τ_{xy}^i) of a fiber section of a RC beam [12], a bi-axial fiber constitutive model is developed according to the Modified Compression Field Theory (MCFT). The steps and mathematical expressions used to calculate the terms entering equilibrium, compatibility and stress-strain relationships are listed in Table 1. For the cross-sectional state-determination the following assumptions were made:

- The longitudinal ε_x and shear γ_{xy} strains are known for each fiber, according to the plane-sections assumption and to a parabolic shear strain distribution along the height of the section with the maximum value $\gamma_{xy.max}$ located on the neutral axis y_{na} (Eq. (2), two half-parabolas with the same maximum are met at the point of neutral axis with different starting point, extreme tensile and extreme compressive fiber respectively).

$$\gamma_{xy}(y) = \gamma_{xy.max} \cdot \left[2\left(\frac{y}{y_{na}}\right) - \left(\frac{y}{y_{na}}\right)^2\right] \quad (2)$$

- The transversal concrete stress f_{cy} was determined for each fiber from equilibrium conditions (zero normal stress n_y was assumed).
- The logical flow chart of the iterative procedure used is illustrated in Fig. 3. The parameter sought is the angle of principal directions assuming coincident principal axes for concrete principal stress and strain. In order to accelerate the convergence of the algorithm to the right value of the angle θ, the initial guess value of the procedure for the angle of inclination of principal stresses/strains (angle of principal axis *2* with respect to *x*-axis) is determined according to the following equation:

$$\theta(y) = \frac{\pi}{4} \cdot \left(\frac{y}{y_{cz}}\right)^3, \quad 0 < y \le y_{cz}$$
$$\theta(y) = \frac{\pi}{4} + \frac{\pi}{4} \cdot \left[2\left(\frac{y-y_{cz}}{y_{tz}}\right) - \left(\frac{y-y_{cz}}{y_{tz}}\right)^2\right], \quad y_{cz} < y \le d \tag{3}$$

where y is the location of the concrete layer/fiber (y : zero reference is the extreme compressive fiber, Fig.6.1), y_{cz} is the depth of the compression zone, y_{tz} is the depth of the tension zone and d is the total depth of the section (i.e., $y_{cz}+y_{tz}=d$, Fig. 1).

Fig. 4 depicts the angle shape function along the height of the section according to the above equation (d =457 mm, y_{cz} = 280 mm similar to Specimen 1 [13]). The solution to the iterative procedure is reached by applying the Regula Falsi root finding a numerical solution [14].

Table 1 - Equations embodied in the iterative procedure [12].

$\varepsilon_x = \varepsilon_{cx}$, $\varepsilon_1 = \varepsilon_x + \frac{\gamma_{xy}\cdot\tan(\pi/2-\theta)}{2}$, $\varepsilon_y = \varepsilon_1 - \frac{\gamma_{xy}}{2\cdot\cdot\tan(\pi/2-\theta)}$, $\varepsilon_2 = \varepsilon_x + \varepsilon_y - \varepsilon_1$
$f_{c1} = E_c \cdot \varepsilon_1$ for $0 < \varepsilon_1 \le \varepsilon_{cr}$, $f_{c1} = \frac{f_{cr}}{1+\sqrt{200\varepsilon_1}}$ for $\varepsilon_{cr} < \varepsilon_1 \le \varepsilon_{yx}$,
$f_{c2} = f_{c2max} \cdot \left[2\left(\frac{\varepsilon_2}{\varepsilon_c'}\right) - \left(\frac{\varepsilon_2}{\varepsilon_c'}\right)^2\right]$, $\frac{f_{c2max}}{f_c'} = \frac{1}{0.8-0.34\varepsilon_1/\varepsilon_c'} \le 1.0$, $f_{sy} = E_{sy}\varepsilon_y \le f_{yy}$
$f_{cy} = -\rho_y \cdot f_{sy}$, $\tau_{xy} = \frac{f_{cy}-f_{c2}}{\tan(\pi/2-\theta)}$, $f_{cx} = f_{c1} - \tau_{xy} \cdot \tan(\pi/2 - \theta)$, $G_{sec} = \frac{\tau_{xy}}{\gamma_{xy}}$,
$E_{sec} = \frac{f_{cx}}{\varepsilon_x}$,
$theta(\varepsilon_{cx}, \gamma_{xy}) = \tan^{-1}\frac{f_{c1}-f_{cy}}{\tau_{xy}}$
f_c'= Concrete Cylinder Compressive Strength (MPa),
ε_c'= Strain at Concrete Cylinder Compressive Strength,
E_c= Concrete Elastic Modulus (MPa),
f_{cr}= Tensile Concrete Strength (MPa),
ε_{cr}= Cracking Strain at attainment of Tensile Concrete Strength,
ε_{yx}= Yielding Strain of Longitudinal Reinforcement,
E_{sy}=Elastic Modulus of Stirrups (MPa),
f_{yy}= Yielding Strength of Stirrups (MPa),
ρ_y= Stirrup Reinforcement Ratio.

2.2 Sectional Model

Fig. 5 depicts a beam element with its degrees of freedom and its displacement/forces in global, local and basic systems of reference. The term "basic" is derived from the system of reference where the rigid body motion of the beam is extracted. Considering now the virtual work principle for the beam element of Fig. 5, the Eq. (4) can be derived. The external work is done by the end forces (p) on the corresponding displacements (u), whereas the internal work is done by the basic forces (q) on the corresponding deformations (v).

$$\delta u^T p = \delta v^T q \tag{4}$$

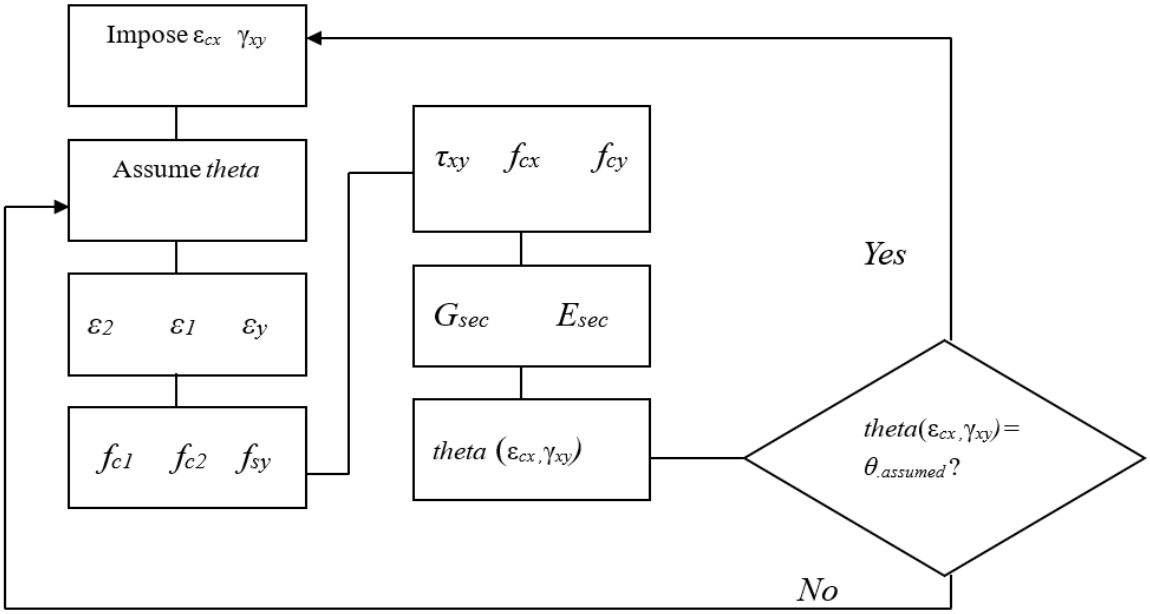

Fig. 3 – Flow Chart of the iterative procedure for each fiber/layer of the section according to MCFT [5], [6].

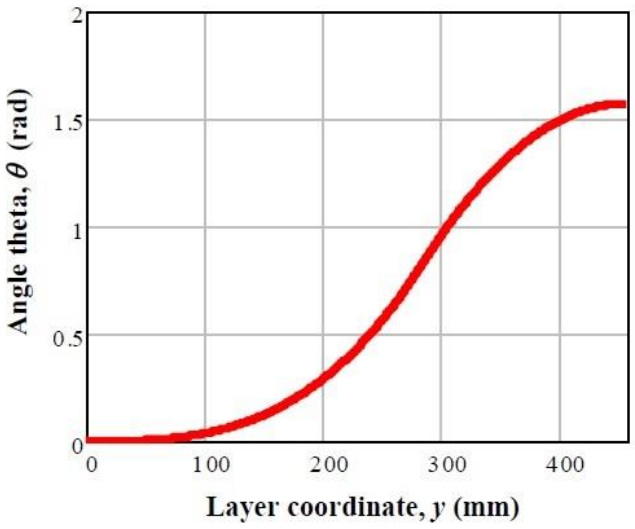

Fig. 4 – Shape function for angle theta (θ) of inclination of principal stresses/strains [5], [6].

The internal work of Eq. (4) can be derived from the integral of the stress product with the corresponding virtual strains over the element volume *V*. In many applications of nonlinear structural analysis, the internal work is limited to the internal work of normal stress σ_x and shear stress τ, on the axial strain ε_x and shear strain γ respectively [1]:

$$\delta v^T q = \int \delta \varepsilon^T \sigma \, dV = \int (\delta \varepsilon_x \, \sigma_x + \delta \gamma \, \tau) dV \tag{5}$$

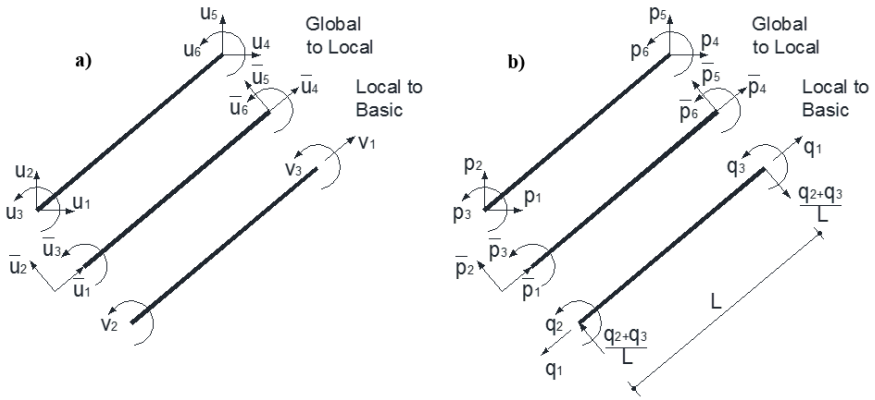

Fig. 5 – Beam a) displacements and b) forces in global, local and basic reference systems [5], [6].

The strain and stress are functions of the position along the element longitudinal axis *x* and the position within the cross section specified in local coordinates *y* (with respect to the height) and *z* (with respect to the width). Eq. (5) can be rewritten by substituting the integral over the element volume by integration over the sectional area *A* at a location *x* followed by integration over the element length:

$$\delta v^T q = \int (\delta\varepsilon_x \, \sigma_x + \delta\gamma \, \tau) dV = \int [\int (\delta\varepsilon_x \, \sigma_x + \delta\gamma \, \tau) dA] \, dx \tag{6}$$

The strains at a fiber/layer point of the beam cross section (*2d* case) are related to the sectional deformations as follows [7]:

$$\varepsilon_x(x) = \varepsilon_0 - y_\varepsilon \cdot \varphi(x) \tag{7}$$

$$\gamma_{xy}(x) = \gamma_{xy.max} \tag{8}$$

where ε_0 is the axial deformation at the center of the coordinate system of the section (center of mass) and y_ε is measured also with reference to this center, $\varphi(x)$ is the curvature of the cross-section and $\gamma_{xy.max}$ is the maximum value of shear strain located on the neutral axis. Therefore, the strains at a material point *m* of the section can be expressed in matrix form as follows:

$$\varepsilon(x, y_\varepsilon) = \begin{Bmatrix} \varepsilon_x \\ \gamma_{xy} \end{Bmatrix} = \begin{bmatrix} 1 & -y_\varepsilon & 0 \\ 0 & 0 & 1 \end{bmatrix} \cdot \begin{Bmatrix} \varepsilon_0 \\ \varphi \\ \gamma_{xy.max} \end{Bmatrix} = B_s(y_\varepsilon) \cdot e(x) \tag{9}$$

$$B_s(y_\varepsilon) = \begin{bmatrix} 1 & -y_\varepsilon & 0 \\ 0 & 0 & 1 \end{bmatrix} \tag{10}$$

The internal resultant forces at the control section are given by:

$$Axial\ force: \quad N = \int \sigma_x dA \tag{11}$$

$$Shear\ force: \quad V = \int \tau_{xy} dA \tag{12}$$

$$Bending\ Moment: \quad M = -\int y_\varepsilon \sigma_x dA \tag{13}$$

These can be written in matrix form as follows:

$$f_s(x) = \int {B_s}^T(y_\varepsilon) \cdot \sigma(x, y_\varepsilon) dA \tag{14}$$

where:

$$f_s(x) = \begin{Bmatrix} N \\ M \\ V \end{Bmatrix},\ B_s(y_\varepsilon) = \begin{bmatrix} 1 & -y_\varepsilon & 0 \\ 0 & 0 & 1 \end{bmatrix},\ \sigma(x, y_\varepsilon) = \begin{Bmatrix} \sigma_x \\ \tau_{xy} \end{Bmatrix} \tag{15}$$

Taking into account the section discretization into fibers/layers, the total forces on the beam section are easily computed through the summation of the individual fiber contributions:

$$N = \sum_{i=1}^{n.layer} \sigma_x^i A^i \quad , \quad V = \sum_{i=1}^{n.layer} \tau_{xy}^i A^i \quad , \quad M = -\sum_{i=1}^{n.layer} \sigma_x^i {y_\varepsilon}^i A^i \tag{16}$$

where A^i is the area of the i-th fiber/layer. Normal and shear stress for the i-th fiber/layer (σ_x^i, τ_{xy}^i) are obtained from the respective strains using a bi-axial fiber constitutive model according to the MCFT (Fig. 3, $\sigma_x^i = f_{cx}^i$). In the employed procedure, the section forces are determined based on known sectional deformations; thus, for known forces, the iterations are conducted over the values of the deformations within a predefined acceptable tolerance for the force magnitudes.

The procedure for calculating the tangent section stiffness matrix k_s is obtained from differentiation of the section force vector f_s with respect to the section deformation vector e:

$$k_s = \begin{bmatrix} \frac{\partial f_{s_1}}{\partial e_1} & \frac{\partial f_{s_1}}{\partial e_2} & \frac{\partial f_{s_1}}{\partial e_3} \\ \frac{\partial f_{s_2}}{\partial e_1} & \frac{\partial f_{s_2}}{\partial e_2} & \frac{\partial f_{s_2}}{\partial e_3} \\ \frac{\partial f_{s_3}}{\partial e_1} & \frac{\partial f_{s_3}}{\partial e_2} & \frac{\partial f_{s_3}}{\partial e_3} \end{bmatrix} \tag{17}$$

$$k_s = \frac{\partial f_s}{\partial e} = \int {B_s}^T(y_\varepsilon) \cdot \frac{d\sigma(x,y)}{\partial \varepsilon(x,y)} \cdot \frac{\partial \varepsilon(x,y)}{\partial e} dA = \int {B_s}^T(y_\varepsilon) \cdot \frac{d\sigma(x,y)}{d\varepsilon(x,y)} B_s(y_\varepsilon) dA \tag{18}$$

$$\sigma(x, y_\varepsilon) = \begin{Bmatrix} \sigma_x \\ \tau_{xy} \end{Bmatrix}\ \varepsilon(x, y_\varepsilon) = \begin{Bmatrix} \varepsilon_x \\ \gamma_{xy} \end{Bmatrix} \tag{19}$$

$$\frac{d\sigma(x,y)}{d\varepsilon(x,y)} = \begin{bmatrix} E_m & 0 \\ 0 & G_m \end{bmatrix} \tag{20}$$

where E_m and G_m are the tangent moduli of the stress – strain relations at a point m of the section approximated here by E_{sec} and G_{sec} (Table 1, Fig. 3).

3. Embedded Pushover Algorithm in Phaethon Software

The simple cantilever column is considered under various load combinations (axial load, moment and shear); this represents the shear-span of an actual column under lateral sway, extending from the support to the point of inflection (i.e. position of zero moment). Although from a statics perspective this is a very simple case, its numerical simulation with all interacting deformation mechanisms is still yet a very challenging task to accomplish. Towards this need and for the case of shear-critical cantilever reinforced concrete columns a computer program was developed to be used as a tool for the study of the mechanics of the nonlinear program

(software "Phaethon"). In the following section the pushover algorithm embodied in this Windows application is presented.

3.1 Pushover Algorithm

For the calculation of the lateral load resistance curve of a column shear span under lateral sway, pushover analysis is conducted: Considering a cantilever shear-critical RC column in Phaethon, the sectional model (either rectangular or circular) established in the previous Section is employed along with the anchorage model in the footing [15],[16] . An increasing lateral point load at the tip of the cantilever is applied (Fig. 6) and a unique fiber element is assigned to the entire height of the cantilever column with the number of Gauss-Lobatto integration points selected by the user. The user also selects the analysis step of lateral load V to be applied in the Pushover analysis, and the total number of steps until maximum load is attained. (Note that the Modified Compression Field Theory in the fiber approach as described by Bentz [17] cannot reproduce the descending branch of shear-critical columns which is why a load-control procedure was selected to be embedded in Phaethon). The maximum load in Phaethon is the load of the last step of convergence of the algorithm in incremental form. It should be highlighted that in reality the shear-critical column's ascending response is followed by a descending branch of progressive failure; however, the proposed algorithm is limited by strength attainment. After peak load, the descending branch of the capacity curve is defined as the line connecting the maximum load point with the point at axial failure; this is quantified in terms of the drift estimate by Elwood and Moehle [18] and 20% of the attained maximum load as residual load at axial failure.

For each point load at the tip of the cantilever (Fig. 6) the corresponding shear force at the assigned column's sections (integration points) is equal to that load (constant shear diagram). The flexural moment at the base of the column, M_0, as well as the moment distribution, are both obtained from the lateral load value (constant shear force). The concentric axial load (tensile or compressive) applied at the tip of the cantilever is also constant throughout the pushover analysis and along the length of the cantilever and therefore each column's section has an axial force value equal to the one applied at the tip. Following this procedure, the vector f_s which is the vector of resisting section forces (see previous Section) should converge to the above defined section forces based on the moment, shear and axial load diagram of the cantilever column under constant axial load and gradually increasing lateral tip point loading.

The following algorithm is applied in Phaethon to achieve this convergence:

Given the externally applied section forces s, i.e. an axial force N, a bending moment M and a shear force V, the equilibrium equation between applied and resisting section forces is set up:

$$s_u(e) = s - f_s(e) = 0 \tag{21}$$

The Newton-Raphson algorithm for the solution of the system of three nonlinear equations is:

1. Given the nonlinear equations $s_u(e) = 0$ and a guess of the solution e_0.

2. For $i = 0 \ldots n$ determine function value $s_u(e_i)$ and derivatives $k_s(e_i)$ (see previous Section).

3. Determine correction to previous solution estimate, $\Delta e_i = s_u(e_i)/k_s$

4. Update the solution estimate: $e_{i+1} = e_i + \Delta e_i$

Return to Step 2 until the error norm is smaller than specified tolerance. On convergence determine the resisting forces for the final deformations.

It should be highlighted that for the cases of "pure compression" or "pure tension" with the angle of inclination of principal stresses/strains (angle of principal axis 2 with respect to x-axis) being zero or $\pi/2$ respectively then no iteration is required, but the fiber state determination is defined from the normal strains,

after referring directly to the uniaxial stress strain laws of the materials (previous Section, Table 1) without calculating any rotation for the principal axes.

After convergence of the section forces is achieved along the length of the cantilever column to the correct values based on the corresponding forces' diagrams along the element due to the applied tip horizontal and axial load, the axial deformation, curvature and shear strain is determined for each section. Integrating the curvatures (Fig. 6) along the shear span of the cantilever column leads to the rotation of the cantilever column due to flexure, which can be easily transformed to lateral displacement due to flexure $\Delta_o{}^f$ by multiplying with the length of the shear span. Integration of the shear strains (Fig. 6) by sampling a few sections (positions defined according with Gauss-Lobatto) along the length of the cantilever column (integration points) leads to the lateral displacement $\Delta_o{}^{sh}$ due to the shear distortion mechanism of the cantilever column. Finally, the rotation and the displacement $\Delta_o{}^{sl}$ due to pull-out of the tensile reinforcement (Fig. 6) is determined based on the closed-form solution of the governing equation of bond [15],[16]. All the above simultaneous contributions (flexure, shear and anchorage) are added together to define the total lateral displacement (i.e., $\Delta_o = \Delta_o{}^f + \Delta_o{}^{sh} + \Delta_o{}^{sl}$) of the cantilever column at each lateral load step and to obtain the capacity curve of the column until maximum lateral load (Fig. 6).

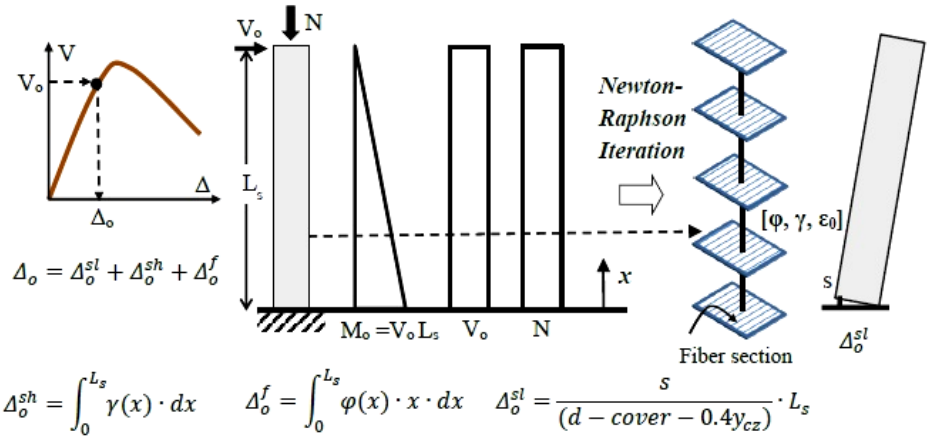

Fig. 6 – Pushover Analysis in Phaethon [5], [6].

4. Correlation with Experimental Results

This section presents the correlation of the shear-flexure capacity curves obtained from the pushover analysis conducted using Phaethon with the experimental response curves of a number of shear-critical RC columns selected from literature (Fig. 7). In the correlation are also included curves obtained from flexural fiber beam/column-based toolbox FEDEAS Lab [19] and from MCFT-based software and dual-section analysis Response 2000 [17]. A satisfactory correlation with experimental results, compared also to what the aforementioned softwares provide, is depicted in Fig. 7 especially in terms of maximum load, degradation stiffness and ultimate lateral displacement.

5. Conclusions

In the present paper a force-based fiber beam-column element accounting for shear effects and the effect of tension stiffening was developed, in order to provide an analytical test-bed for simulation and improved understanding of experimental cases where testing of reinforced concrete columns actually led to collapse. The developed fiber-element is incorporated in the stand-alone Windows program Phaethon with user's interface written in C++ programming language code that offers the possibility to its user to obtain the capacity curve for shear-critical reinforced concrete cantilever columns taking into account shear – flexure interaction mechanism but also of the important contribution in the final column's lateral displacement, of the pull-out of the inadequate anchorage of the tensile longitudinal reinforcing bars of the column. This is available for both

rectangular but also circular reinforced concrete columns. In addition, the software resolves strain, slip and bond distributions along anchorage length. Comparison with experimental results from the literature verifies the capability of this Windows software tool to assess strength and deformation indices of shear-critical reinforced concrete columns. Finally, the moment curvature but also the shear force – shear strain analysis of the sections of these columns is also possible, all based on the Modified Compression Field Theory.

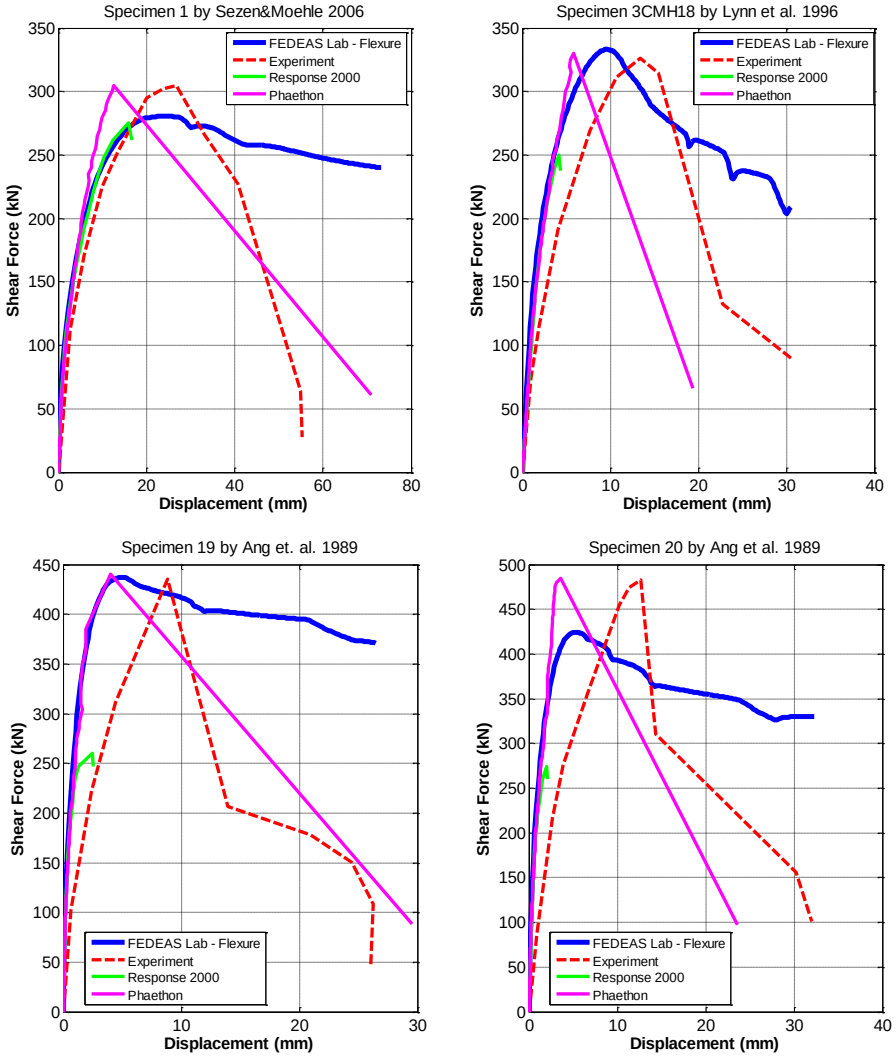

Fig. 7 – Comparison of the capacity curves provided by Phaethon and other software with the experimental responses [13],[20],[21].

6. Acknowledgements

The author would like to thank the Alexander S. Onassis Public Benefit Foundation whose financial support is greatly appreciated. The Phaethon software installation file is available for free on Researchgate DOI: https://doi.org/10.13140/RG.2.2.31114.57284 and its source code is open for download on Github: https://github.com/bigeconomy/Phaethon-Source-Files .

7. References

[1] Filippou, F. C., and Fenves, G. L. (2004): Methods of analysis for earthquake-resistant structures. In: Bozorgnia Y, Bertero VV (eds) *Earthquake engineering: From engineering seismology to performance-based engineering*. CRC Press, Boca Raton.

[2] Mergos, P. E. and Kappos, A. J. (2008): A distributed shear and flexural flexibility model with shear–flexure interaction for R/C members subjected to seismic loading. *Earthquake Engng. Struct. Dyn*., **37**, 1349-1370.

[3] Ceresa, P., Petrini, L., and Pinho, R. (2007): Flexure-shear fiber beam-column elements for modeling frame structures under seismic loading-state of the art. *Journal of Earthquake Engineering*, **11**, 46–88.

[4] Hughes, T. J. R. (2000). *The Finite Element Method: Linear Static and Dynamic Finite Element Analysis*, Dover Publications.

[5] Megalooikonomou K.G. (2019): *Seismic Assessment and Retrofit of Reinforced Concrete Columns*, Cambridge Scholars Publishing, ISBN (10): 1-5275-2785-9, ISBN (13): 978-1-5275-2785-0, p. 387.

[6] Megalooikonomou K.G. (2018): PHAETHON: Software for Analysis of Shear-Critical Reinforced Concrete Columns, *Modern Applied Science*, **12** (3), 1-22.

[7] Ceresa, P., Petrini, L., and Pinho, R. (2008): *A fibre flexure–shear model for cyclic nonlinear behavior of RC structural elements*. Research Report ROSE-2008/07. IUSS Press: Pavia, Italy.

[8] Collins, M. P. (1978): Towards a rational theory for RC members in shear. *ASCE Journal of Structural Division*, **104**(4), 649-666.

[9] Collins, M. P., Vecchio, F. J., and Mehlhorn, G. (1985): An international competition to predict the response of reinforced concrete panels. *Canadian Journal of Civil Engineering*, **12**, 624-644.

[10] Vecchio, F. J., and Collins, M. P. (1982): *Response of Reinforced Concrete to In-Plane Shear and Normal Stresses*, Publication No. 82-03, Department of Civil Engineering, University of Toronto, Canada.

[11] Vecchio, F. J., and Collins, M. P. (1986): The modified compression field theory for reinforced concrete elements subjected to shear. *ACI Journal Proceedings*, **83**(2), 219-231.

[12] Vecchio, F. J., and Collins, M. P. (1988): Predicting the Response of Reinforced Concrete Beams Subjected to Shear Using Modified Compression Field Theory. *ACI Structural Journal*, **85**(3), 258-268.

[13] Sezen, H., and Moehle, J. P. (2006): Seismic Tests of Concrete Columns with Light Transverse Reinforcement. *ACI Structural Journal*, **103**(6), 842-849.

[14] Jean-Luc Chabert, ed. (1999): *A History of Algorithms: From the Pebble to the Microchip*, Berlin: Springer, pp. 86-91.

[15] Megalooikonomou, K. G., Tastani, S. P., and Pantazopoulou, S. J. (2018): Effect of Yield Penetration on Column Plastic Hinge Length. *Engineering Structures, Elsevier*, **156,** 161-174.

[16] Tastani, S. P., and Pantazopoulou, S. J. (2013): Reinforcement and concrete bond: State determination along the development length. *ASCE J. of Structural Eng.*, **139**(9), 1567-1581.

[17] Bentz, E. C. (2000): *Sectional Analysis of Reinforced Concrete Members*. PhD Thesis, Department of Civil Engineering, University of Toronto, Toronto, Canada.

[18] Elwood, K. J., and Moehle, J. P. (2005): Axial Capacity Model for Shear-Damaged Columns. *ACI Structural Journal*, **102**(4), 578-587.

[19] Filippou, F. C., and Constantinides, M. (2004): FEDEAS Lab – Getting Started Guide and Simulation Examples, *NEESgrid Report 2004-22* and *SEMM Report 2004-05*.

[20] Ang, B. G., Priestley, M. J. N., and Paulay, T. (1989): Seismic Shear Strength of Circular Reinforced Concrete Columns. *ACI Structural Journal*, **86**(1), 45-59.

[21] Lynn, A. C., Moehle, J. P., Mahin, S. A., and Holmes, W. T. (1996): Seismic Evaluation of Existing Reinforced Concrete Columns. *Earthquake Spectra*, **12**(4), 715-739.